Available online at www.sciencedirect.com
ScienceDirect
Catalysis Today 123 (2007) 142–150
CATALYSIS TODAY
www.elsevier.com/locate/cattod

# Hydrogenation of 3,4-epoxy-1-butene over Cu–Pd/$SiO_2$ catalysts prepared by electroless deposition

Melanie T. Schaal, Ashley Y. Metcalf, Joseph H. Montoya, J. Paul Wilkinson, Carol C. Stork, Christopher T. Williams, John R. Monnier *

*Department of Chemical Engineering, Swearingen Engineering Center, University of South Carolina, Columbia, SC 29208, United States*

Available online 23 January 2007

**Abstract**

Electroless deposition has been used to prepare Cu–Pd/$SiO_2$ bimetallic catalysts wherein initial Cu coverages are limited only to the pre-existing Pd surface. Cu loading on the Pd surface can be systematically varied by modification of deposition kinetic parameters. In this case deposition time was used as the kinetic variable for the preparation of a series of Cu–Pd catalysts. These materials have been characterized using atomic absorption, CO chemisorption, and FT-IR (adsorption of CO), and then evaluated for the hydrogenation of 3,4-epoxy-1-butene, a functionalized olefin having many potential reaction pathways. Catalyst performance and characterization results suggest that Cu is not distributed in a monodisperse manner on the Pd surface, indicating the existence of autocatalytic deposition of Cu on Cu sites. The FT-IR results suggest that although CO adsorption on all sites is suppressed by Cu addition, initial Cu deposition occurs more readily on certain sites. The bimetallic Cu–Pd sites that are formed exhibit unusually high activity for EpB conversion and formation of unsaturated alcohols and aldehydes. This bimetallic effect on catalyst activity and selectivity is best explained, not by the existence of either ligand or ensemble effects, but rather by the bifunctional nature of the Cu–Pd sites present on the surface of these catalysts.


*Keywords:* Hydrogenation; Multi-functional olefins; 3,4-Epoxy-1-butene; Epoxybutane; Electroless deposition; Bimetallic catalysts; Copper; Palladium

## 1. Introduction

Platinum group metal (PGM) catalysts are typically used in the selective hydrogenation of functionalized olefins [1–3], such as those that contain both C=C bonds and reductive C–O moieties. For example, during the hydrogenation of unsaturated aldehydes or ketones, it is sometimes desirable to selectively hydrogenate only the C=C bond to form the saturated ketone or aldehyde, while in other cases the preferred reaction pathway might involve only the reduction of the C=O bond to form the corresponding unsaturated alcohol [4,5]. The hydrogenation of 3,4-epoxy-1-butene (EpB) is another example of where different reaction pathways can lead to a variety of reaction products, since this molecule contains two distinct functional groups, a C=C double bond and an epoxide ring. Epoxybutane is the reaction product for the selective hydrogenation of the C=C bond; however, hydrogenolysis/hydrogenation of the epoxide ring can lead to the formation of both saturated and unsaturated alcohols and aldehydes. For instance, Bartok et al. [6] have studied the hydrogenation of 3,4-epoxy-1-butene over Pt/$SiO_2$ and Pd/$SiO_2$ catalysts and found that for Pt the principal oxygenated products were 1,2-epoxybutane (butylene oxide or BO) with lesser amounts of butanal (*n*-butyraldehyde); significant levels of $C_4$ hydrocarbons, formed by the deoxygenation of EpB to butadiene, and ultimately hydrogenation to butenes and butane, were also observed. For Pd/$SiO_2$, epoxybutane, butanal, 2-butenal (crotonaldehyde), and 3-methoxypropene were all observed. Thus, for both catalysts, the hydrogenation of EpB was non-selective; both direct hydrogenation and hydrogenolysis/hydrogenation reaction pathways were evident. For EpB hydrogenation over Cu/$SiO_2$ catalysts, Bartok et al. [7] observed that butene isomers were formed when the copper was present as $Cu^0$; however, when copper was present as both Cu metal and Cu(I) oxide, isomerization to 2-butenal and 2,5-dihydrofuran represented the predominant pathways. In a related study, Hubaut et al. [8] investigated the hydrogenation of 2-butenal over Cu/$Cr_2O_3$ catalysts and found that *n*-butanal (hydrogenation of C=C bond) and 2-buten-1-ol

* Corresponding author. Tel.: +1 803 777 9543; fax: +1 803 777 8265.
*E-mail address:* monnier@engr.sc.edu (J.R. Monnier).

0920-5861/$ – see front matter 
doi:10.1016/j.cattod.2007.01.015

(hydrogenation of C=O bond) were the primary products. Using a different platinum group metal, Monnier and coworkers [9,10] and Falling [11] tested $Rh/SiO_2$ catalysts for the selective hydrogenation of EpB and observed that while epoxybutane was the selective product, lesser, but significant, amounts of *n*-butanol and *n*-butanal were also formed. The latter two products were formed by the hydrogenation of 2-buten-1-ol (crotyl alcohol) and 2-butenal, respectively. Batch kinetic data analyses showed that for the Rh-catalyzed hydrogenation of EpB there was a three-pronged parallel reaction pathway; epoxybutane, *n*-butanol, and *n*-butanal were the stable, end products of each of the three reaction pathways. Even homogeneous catalysts which typically exhibit higher selectivities than their heterogeneous counterparts are non-selective for EpB hydrogenation. Fujitsu et al. [12] and Alper and coworkers [13] have utilized Rh(I) complexes and Pd(I) complexes, respectively, for the catalytic hydrogenation of EpB and observed that the normally more selective organometallic complex catalysts gave the same variety of products as seen for heterogeneous catalysts.

One potential way to modify reaction pathways for hydrogenation of bifunctional olefins is to use bimetallic catalyst compositions. Much has been written [14–18] about the possible roles of ligand and ensemble effects in bimetallic catalysts shifting reaction pathways, particularly for reactions that are considered to be structure sensitive, where specific reaction rates and/or product distributions change with surface composition of the catalyst. Ensemble effects are defined in terms of the number of contiguous surface atoms needed for a particular catalytic reaction to occur. Catalytic reactions such as simple C=C bond hydrogenation are considered to be structure insensitive, since this reaction is considered to occur on as few as 1–4 contiguous surface atoms. Catalytic hydrogenolysis of C–C or C–O bonds are often believed to be structure sensitive, since either more sites, or combinations of more energetic sites, are needed for these reactions to take place. Ligand effects refer to those modifications in catalytic activity or selectivity that are the result of electronic interactions between the components of the bimetallic system. Again, hydrogenation of simple olefins would not be considered to be sensitive to ligand effects, while hydrogenolysis reactions that require more energetic sites would be sensitive to the electronic interactions between the bimetallic components to change activity or selectivity.

However, in spite of the potential importance of bimetallic catalysts in changing reaction rates or pathways, preparation of true bimetallic catalyst compositions is not straightforward. Bimetallic catalyst synthesis is typically carried out by either simultaneous co-impregnation of both metal salts onto a catalyst support or by successive steps of metal salt addition. For either of these preparative methods, it is virtually impossible to ensure formation of only bimetallic particles; rather, formation of separate metallic particles of both metals can and does occur [19,20]. Thus, it is very difficult to characterize such catalytic systems, and even more difficult to correlate catalyst performance with bimetallic catalyst composition. An alternative approach for the preparation of bimetallic catalysts is the use of electroless deposition (ED) of reducible metal salts onto other metals [21–23]. Electroless deposition has been used extensively in modern technology in fields such as electronics, corrosion protection, batteries, and biomedical applications, but rarely in the preparation of novel, bimetallic catalysts. ED is a catalytic or autocatalytic process for the deposition of metallic components by a controlled chemical reaction that is catalyzed by the pre-existing metal (catalysis) or the metal which is being deposited (auto-catalysis). In principle, all metals that can be deposited using electrodeposition can also be deposited using ED, without the difficulties of maintaining electrical conductivity, which is required in conventional electrochemistry. Almost all previous work has been focused on preparing thick, continuous metal films on appropriate substrates, not for the preparation of bimetallic catalyst particles, where the desire is to prepare a particle having a surface containing both metallic components. However, the application of ED in preparing bimetallic particles uses the same principles employed in the formation of thick films, except that reaction conditions must be tailored to deposit only small, controlled amounts of the reducible metal ion ($M^{n+}$) onto the surface of pre-existing, catalytic metal particles. Since ED itself obeys simple kinetics, $M^{n+}$ deposition is dependent upon solution temperature, $M^{n+}$ concentration, concentration of reducing agent (typically, $BH_4^-$, substituted amine boranes, formaldehyde, or $H_2PO_2^-$), and concentration of catalytic surface. The addition of other agents, such as organic acids or salts of organic acids, can further stabilize the $M^{n+}$ solution against uncontrolled reduction.

Since deposition of $M^{n+}$ is limited to the catalyst already present on the support, only bimetallic particles are formed. For example, Gauthard et al. [24] and Melendrez et al. [25] have studied the catalytic reduction of aqueous $NO_3^{2-}$ and selective hydrogenation of *o*-xylene, respectively, using supported, bimetallic Cu–Pd catalysts prepared by the electroless deposition of $Cu^{2+}$ salts onto Pd surfaces (gaseous $H_2$ used as the reducing agent during catalyst preparation). Both authors claimed that the existence of discrete Cu–Pd particles gave rise to catalyst performance different from bimetallic catalysts prepared by simultaneous impregnation of both $Cu^{2+}$ and $Pd^{2+}$ salts onto a support. Infrared analyses of CO adsorbed on the Cu–Pd surfaces were used to infer the existence of bimetallic Cu–Pd particles. Chang et al. [26] have prepared $Cu/Al_2O_3$ catalysts by the electroless deposition of $Cu^{2+}$, using aqueous formaldehyde (HCHO) as the reducing agent, onto an $Al_2O_3$ surface that had been previously seeded with Pd nuclei (by impregnation of $PdCl_2$, followed by calcination and reduction). Palladium functioned as the catalyst for the activation of the HCHO reducing agent, which served as the site for $Cu^0$ deposition. The level of deposition of Cu was high enough that the amount of Pd was negligible in the final catalyst. The benefit of the $Cu/Al_2O_3$ catalyst prepared in this manner was that Cu crystallite diameters remained essentially constant at 4.0–5.0 nm up to approximately 15 wt.% Cu, since the pre-seeded Pd sites acted as the sole nucleation sites for Cu particle formation. The authors observed that these catalysts were more active for isopropanol and cyclohexanol dehydrogenation to acetone and cyclohexanone, respectively, than conventional

supported Cu catalysts, since the more highly dispersed Cu crystallites had higher exposed Cu site concentrations.

In this paper, we present preliminary data for the selective hydrogenation of EpB over $Pd/SiO_2$ catalysts that have been modified by the addition of different amounts of copper, whereby the copper has been deposited on the Pd surface using electroless deposition methodologies. The goals of this paper are not only to discuss the subsequent improvements in catalyst performance and selectivity during EpB hydrogenation, but also to illustrate the potential of electroless deposition methods as a way to prepare viable, bimetallic catalysts for use in large-scale, chemical catalysis.

## 2. Experimental methods

### 2.1. Catalyst preparation

The base 2.0 wt.% $Pd/SiO_2$ catalyst was supplied by Engelhard Corporation. Characterization by CO chemisorption gave an average Pd dispersion of 0.25 (Pd crystallite diameter calculated to be 4.4 nm), which corresponded to a surface Pd site concentration of $4.70 \times 10^{-5}$ mol/$g_{cat}$, or $2.8 \times 10^{19}$ surf Pd/$g_{cat}$. The surface area of the non-acidic $SiO_2$ support was reported as 45–60 $m^2$/g. The addition of different loadings of Cu to the Pd surface was conducted by electroless deposition using the following sequence. Approximately 25 g of the base $Pd/SiO_2$ catalyst was pretreated in a flowing stream of 20% $H_2$, balance He (GHSV = 1000 $h^{-1}$) at 473 K for 2 h, to ensure complete reduction of the Pd crystallites. Following this reduction procedure, the sample was stored *in vacuo* in a moisture-free desiccator. Portions of this master sample were then used for all subsequent ED treatments. All electroless deposition baths were prepared using appropriate amounts of $Cu(NO_3)_2$ as the source of $Cu^{2+}$, the Na salt of EDTA as the $Cu^{2+}$ stabilizing agent, 37% aqueous formaldehyde (HCHO) as the reducing agent, and NaOH as needed to adjust the initial pH of the solution to 12.5. The effect of pH on the integrity of the silica stars was investigated at pH 12.5 and showed no dissolution or visible structural degradation over periods of time greater than those used for the ED experiments in this study. The total volumes of all ED baths were maintained at 20 mL; the actual ED experiments were conducted in single-use polypropylene cups to minimize the possibility of wall-enhanced, thermal reduction of the ED solutions. After the ED bath was assembled, 0.2 g of the reduced $Pd/SiO_2$ catalyst were added and the polypropylene cup was placed on a swivel plate to agitate the solution. The extent of copper deposition was controlled by the length of time the catalysts were immersed in the bath, varying from 2 to 60 min. After the catalysts had been in the solution for the specified time, the solution was rapidly filtered, and the catalysts were rinsed thoroughly with deionized water. Finally small portions of the catalysts were analyzed using atomic absorption (Perkin Elmer, Model 3300) to determine the weight percent of copper deposited on the catalyst.

A 2 wt.% $Cu/SiO_2$ catalyst was prepared by traditional incipient wetness methodologies using $Cu(NO_3)_2$. The monometallic Cu catalyst was reduced at 573 K in flowing $H_2$ (instead of 473 K) to ensure complete reduction since this sample was not exposed to formaldehyde.

### 2.2. Catalyst characterization

Carbon monoxide chemisorption was performed using a Quantochrome Autosorb 1 chemisorption analyzer. Samples were pretreated in flowing $H_2$ at 473 K for 2 h followed by evacuation at 473 K for 2 h. Chemisorption was conducted at 313 K over the pressure range 50–300 Torr of CO. A 1:1 CO to Pd adsorption stoichiometry was used, as assumed by others for $Pd/SiO_2$ [27]; $Cu^0$ was considered to be inactive for CO chemisorption [28,29]. Unless otherwise noted, monolayer (ML) Cu coverage on Pd was calculated as shown below:

$$\theta_{Cu} = \frac{(\text{CO uptake for Pd/SiO}_2 - \text{CO uptake for Cu–Pd/SiO}_2)}{\text{CO uptake for Pd/SiO}_2} \quad (1)$$

For Fourier transfer infrared (FT-IR) measurements, pellets of 1.27 cm diameter were prepared by pressing ~0.015 g of ground sample at 4500 lb force (~20,000 N). Spectra were obtained using a Thermo Electron model 4700 spectrometer with a liquid nitrogen cooled MCT detector. Experiments were conducted in a cylindrical cell containing entrance and exit ports such that the ~70 mL/min total gas flow passed either through or around the pellet. Heating was conducted using a heating tape wrapped around the cell and was controlled using a conventional temperature controller. Samples were pretreated *in situ* at 473 K ($Cu/SiO_2$ pretreated at 573 K) in flowing $H_2$ (UHP grade) for 1 h and then cooled to room temperature in He (UHP grade). For each pellet, a background spectrum in flowing He was taken and subtracted from all subsequent spectra. The pellet was then exposed to 1% CO/balance He flow for 15–20 min followed by 100% He flow to remove gas phase and physisorbed CO. The FT-IR spectra were then taken in the automatic gain mode using 64 scans at 2 $cm^{-1}$ resolution. Spectra presented here have undergone spectral subtraction and smoothing as needed to remove noise due to water, although the peak shapes were carefully maintained throughout. Spectral fitting using PeakSolve software was performed on baseline corrected samples.

### 2.3. Catalyst evaluation

Catalysts were evaluated using a single pass, flow reactor system that has been described in earlier reports [30,31]. The feed stream typically consisted of 2.5% EpB, 10% $H_2$, and balance helium. The $H_2$ and He components were added using Tylan mass flow controllers, while a thermostatically-jacketed, stainless steel saturator was used to add the desired flow of EpB vapor to the gas stream. Helium was used as the sweep gas for the saturator, and the saturator was maintained at the desired temperature by recirculation of a $H_2O$/ethylene glycol mixture through the saturator jacket from a closed cycle refrigeration/heater bath. Concentrations as low as 0.1% and as high as

25 mol% EpB could easily be formulated using this feed system. Following *in situ* reduction at 373 K in a gas stream of 20% $H_2$, balance He for 1 h, the catalysts were evaluated for EpB hydrogenation activities. The reaction temperature during EpB hydrogenation was maintained at 323 K at a GHSV of 320,000 $h^{-1}$. The small amounts of catalyst used in these evaluations required dilution of the catalyst with 0.25 g of 40–60 mesh $SiO_2$ support to maintain adequate bed depth. The reactor used in this study was constructed of Pyrex (0.25 in. i.d.); a thermocouple embedded within the catalyst bed was used to monitor reaction temperature. Both the feed and reaction product gas streams could be passed through a gas sample loop in a switching valve assembly, which was directly interfaced with a Hewlett-Packard 5890 gas chromatograph. Products were separated by a 30m Poraplot Q capillary GC column and reactor effluents could be analyzed by either thermal conductivity or flame ionization detection.

## 3. Results and discussion

Before the study of electroless deposition of $Cu^0$ on the Pd/$SiO_2$ catalysts was initiated, thermal stabilities of the various ED solutions were conducted to ensure that the Cu did not precipitate from solution at the ED bath conditions used in this study. All ED solutions, regardless of composition, showed no visible signs (darkening of ED solution) of thermal reduction at 296 K over approximately a 60 min time interval; the ED solutions at 323 and 353 K showed signs of thermal instabilities after approximately 10 and 6 min, respectively. Thermal stabilities of ED baths having higher concentrations of $Cu^{2+}$ and HCHO typically were slightly lower at 323 and 353 K. Further, in all instances, thermal stabilities of all ED solutions were dependent upon the concentration of HCHO, indicating that HCHO was the chemical reducing agent for $Cu^{2+}$ to $Cu^0$. Finally, in all cases, no deposition of $Cu^0$ on the $SiO_2$ support was observed, indicating that Cu deposition was catalyzed by and limited to the Pd present on the $SiO_2$ support.

Based on literature [32,33] data for typical $Cu^{2+}$ ED baths, the following ED bath (denoted as composition 1×) was chosen as the standard composition: $Cu(NO_3)_2$ = 0.0032 M, HCHO = 0.0074 M, NaEDTA = 0.0054 M, and NaOH as needed to adjust pH to 12.5. The aqueous HCHO solution was added to the balance of the ED solution immediately before deposition experiments were begun. In all cases, 20 mL of ED solution was used for 0.200 g Pd/$SiO_2$ catalyst. The effects of deposition temperatures of 296 and 323 K at three different ED bath concentrations (1×, 5×, and 10×) are summarized in Fig. 1. Baths of 5× and 10× concentrations have all molar concentrations multiplied by 5 and 10 times, respectively, relative to the standard 1× bath. Deposition times in Fig. 1 were limited to include only those times where the baths exhibited thermal stability. As stated earlier, higher temperatures and higher concentrations of bath components resulted in shorter periods of thermal stability. Note also that for complete deposition of Cu at 1×, 5×, and 10× bath concentrations, Cu weight loadings correspond to 1.99, 9.23, and 16.90 wt.%, respectively. Thus, all the data in Fig. 1 correspond to <10%

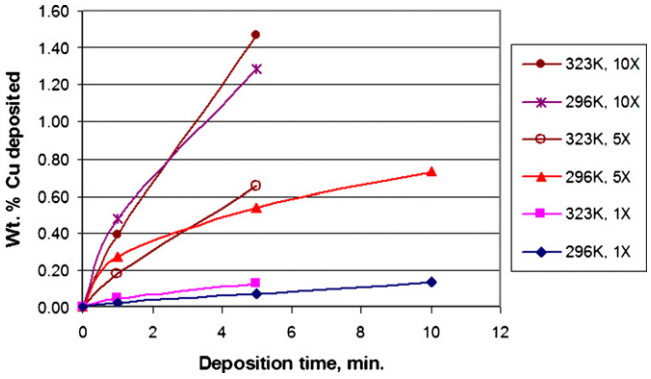


Fig. 1. Effects of temperature and ED bath concentrations on deposition of Cu on Pd/$SiO_2$. In the legend, the first number is the deposition temperature and the second is the concentration of the bath components.

deposition of the Cu present in each of the baths. The deposition curves in Fig. 1 indicate that, while increasing deposition temperature from 296 to 323 K does result in slightly higher rates of Cu deposition, the concentrations of the ED bath components are significantly more important in controlling the rates of Cu deposition. These results are in general agreement with Molenaar et al. [34], who found that Cu deposition on various metal surfaces was more dependent upon the concentrations of $Cu^{2+}$ and HCHO than the temperature of deposition.

Since the goal of this study was to prepare catalysts having low and well-controlled coverages of Cu on the Pd surface, two other ED experiments were conducted to determine the rates of Cu deposition on Pd at even lower Cu concentrations. Electroless developer baths of 0.2× and 0.5× standard composition (with the exception of the HCHO concentration) were prepared and tested at 296 K for Cu deposition. Realizing from the data in Fig. 1 that deposition of Cu would be considerably lower for these two compositions, the concentrations of HCHO reducing agents were varied in these experiments. The results are summarized in Figs. 2 and 3 for the ED bath concentrations 0.2× and 0.5×, respectively. The molar concentrations of HCHO are shown in the legends accompanying each figure. For the composition 0.2×, there was

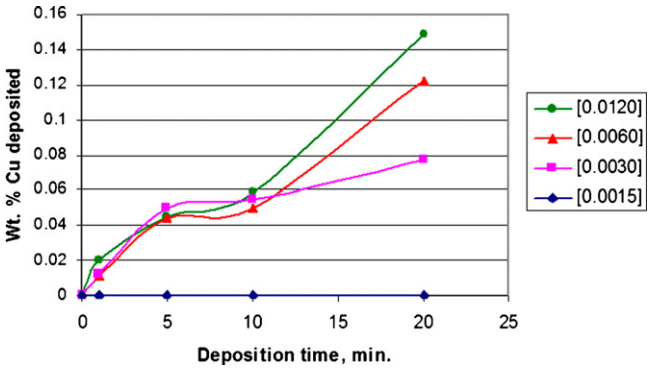


Fig. 2. Deposition of Cu at 296 K as a function of HCHO concentration. Base concentration of ED bath is 0.2× with molar concentration of HCHO as shown in legend. Complete deposition of Cu corresponds to 0.40 wt.% Cu on the Cu–Pd/$SiO_2$ catalyst.

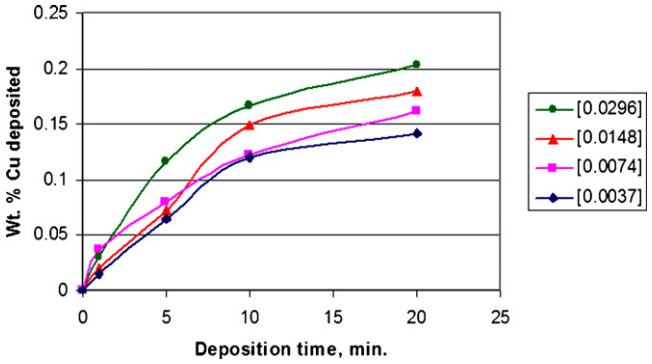


Fig. 3. Deposition of Cu at 296 K as a function of HCHO concentration. Base concentration of ED bath is 0.5× with molar concentration of HCHO as shown in legend. Complete deposition of Cu corresponds to 1.00 wt.% Cu on the Cu–Pd/$SiO_2$ catalyst.

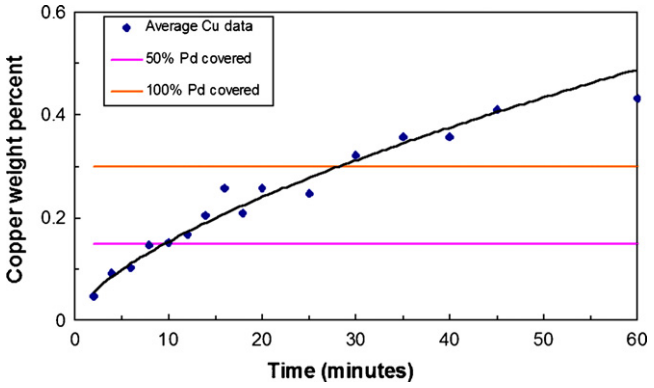


Fig. 5. Copper weight loadings of Cu–Pd/$SiO_2$ catalysts as a function of deposition time. ED solution is 1× concentration and temperature is 296 K.

no measurable deposition even after 60 min when the HCHO was 0.0015 M. Only at higher HCHO concentrations was Cu deposition observed. In general, the higher concentrations of HCHO gave somewhat higher rates of Cu deposition, although the kinetic dependencies were not large. This observation is consistent with the results of others [35,36], who have found that beyond critical concentrations of HCHO in ED solutions, the effect of HCHO concentrations on the rate of Cu deposition is minimal, due to limited accessibility of HCHO (or its basic, aqueous analog, methylene glycol) at the catalytic site (Pd, in our case), where H transfer occurs. The kinetic dependency of $Cu^{2+}$ concentrations on the rate of electroless deposition was not determined for any of the bath compositions, since the $Cu^{2+}$ concentrations used in the preparation of bimetallic catalysts were purposely kept low to give only limited coverages of Cu on the Pd surface.

The data summarized in Fig. 4 show the effects of different bath concentrations on the amounts of Cu deposited at 296 K. A copper weight loading of 0.30 wt.% corresponds to 100% coverage of the Pd surface, assuming monodisperse distribution of Cu on the Pd surface. The batch composition of 1× was selected, since it gave a slow enough deposition of Cu on the Pd surface to permit using deposition time as the variable controlling extent of Cu deposition. The 5× and 10× ED solutions were not considered, since both solutions gave greater than 100% theoretical Cu coverage on Pd, even after 5 min of deposition. Theoretical depositions greater than 100% monodisperse coverage suggest that multilayer coverage of Cu occurs for high levels of Cu deposition (autocatalytic ED). The data in Fig. 5 correspond to the Cu–Pd/$SiO_2$ samples that were prepared for evaluation in our EpB hydrogenation studies. Again, assuming monodisperse Cu coverage, 50 and 100% Cu coverage on Pd occurred at copper weight loadings of 0.15 and 0.30%, respectively.

CO chemisorption results are shown in Fig. 6. As Cu loading increases, μmol CO adsorbed/gram catalyst decreases, confirming that Cu is being deposited on surface Pd sites. The vertical line on the figure indicates where 1 ML coverage of Cu on Pd should be achieved, again assuming monodisperse Cu coverage. Since there is measurable CO chemisorption at this point, it is evident that autocatalytic deposition of Cu on Cu surfaces also occurs. This autocatalytic deposition was expected since metallurgy industries routinely use Cu/formaldehyde ED baths to attain Cu coatings that are several microns thick [33,37].

The adsorption of CO on Cu–Pd catalysts was also examined using FT-IR spectroscopy. Representative spectra for various Cu loadings are shown in Fig. 7. The FT-IR spectrum for Cu/$SiO_2$

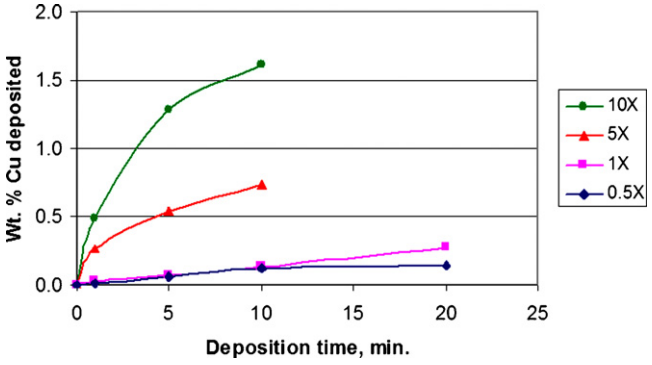


Fig. 4. Cu deposition at 296 K for a series of ED solutions. Assuming monodisperse coverage of Cu on the Pd surface, 0.30 wt.% Cu corresponds to a monolayer coverage of Cu.

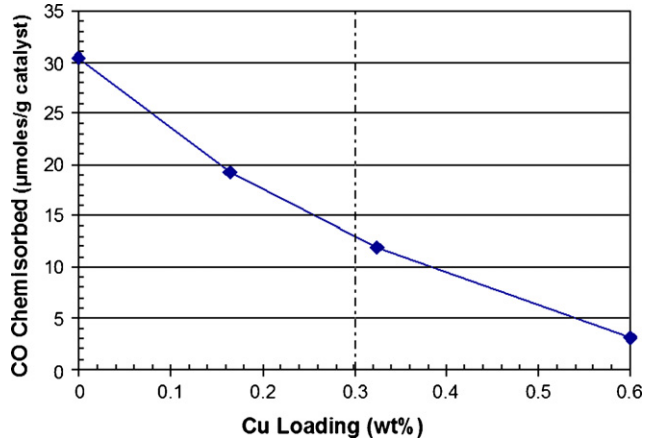


Fig. 6. Pd chemisorption results are shown as μmol CO chemisorbed/gram catalyst. The CO uptake changes as a function of Cu weight loading.

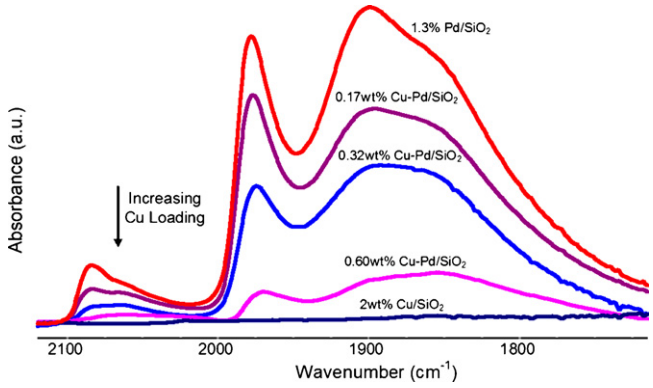


Fig. 7. FT-IR spectra for CO adsorption on $Pd/SiO_2$ and various Cu–Pd bimetallic catalysts. CO adsorption occurred only on the Pd sites; Cu was not active for CO adsorption at these conditions. The spectra corresponding to 0.17 and 0.32 wt.% $Cu–Pd/SiO_2$ were scaled slightly in order to make the trends more apparent.

indicates that CO is not strongly adsorbed on $Cu^0$, consistent with the observations of Skoda et al. [38]. As expected, the increase in Cu loading results in the decrease of CO adsorption on the remaining surface Pd sites, as observed by others [25].

The FT-IR spectra were deconvoluted to provide a more clear understanding of the effects of Cu addition. As shown in Table 1, the deconvolution was fitted to give five different CO adsorption peaks with peak maxima consistent with published results. The data show that as Cu weight loading increases, the CO adsorption peaks shift to lower frequencies. This downshift has been observed by others [42] and has been attributed to lower dipole interactions between neighboring carbonyl species as Cu dilutes the Pd surface into smaller ensembles [42].

The region from 1750 or 1800 to 1900 $cm^{-1}$ is generally assigned to CO adsorption on three-fold hollow sites [39,40]. However, recent experimental and theoretical results have shown CO adsorption on three-fold hollow sites as high as 1920 $cm^{-1}$ [41]. More specifically, when a representative CO adsorption spectrum was deconvoluted using three Gaussian peaks in the 1800–1920 $cm^{-1}$ region, the peaks were centered at 1815, 1882, and 1913 $cm^{-1}$, which is similar to the Pd(1 1 1) peaks reported by Gieβel [43]. Thus, the 1800–1920 $cm^{-1}$ peaks in this study are assigned to CO adsorption on three-fold hollow Pd(1 1 1) sites. The broad nature of peaks in this region, which has been reported by others [40,44], may be partially responsible for the observed variation in wavenumbers.

The region from 1900 to 2050 $cm^{-1}$ is often attributed to two-fold, bridged CO adsorption [39,40]. More specifically, this region has been assigned to two-fold, bridge-bonded CO on Pd(1 0 0 ) surfaces (1895–1997 $cm^{-1}$ for CO coverages up to 0.8 ML) [39], on Pd(2 1 0) surfaces (1878–1996 $cm^{-1}$) [45], on defect-rich Pd(1 1 1) step/kink surfaces (1980–1990 $cm^{-1}$) [41], and on Pd(1 1 0) surfaces (~1985 $cm^{-1}$) [41]. Due to the extensive overlap of possible designations in this area of the IR spectrum, finite peak assignments are very difficult without knowledge of the Pd surface structure.

Finally, the region from 2000 or 2050–2100 or 2150 $cm^{-1}$ is generally assigned to linearly bonded CO on Pd [39,40]. More specifically, Bertarione et al. [46] assigned the peak at ~2070 $cm^{-1}$ to sites such as those existing at corners and step edges that favor stronger back bonding, which results in weaker C–O bonds and lower stretching frequencies [39,47]. Thus, the low frequency linear peak (2032–2074 $cm^{-1}$) has been assigned to CO bonded to low coordination Pd sites [25,39]. The linear peak near 2085 $cm^{-1}$ has also been assigned to step or defect sites [48]. The presence of CO adsorbed to edge/corner sites is expected in this study since for Pd particles with diameters of 44 Å, the statistical models of Van Hardeveld and Hartog [49] predict that between 20 and ~40% of the surface sites are edges and corners.

Although specific peak assignments have been postulated, such assignments are somewhat tentative since CO adsorption on Pd has been reported to vary with CO coverage [46], CO adsorption temperature [50], Pd particle size, and particle morphology [51].

Since quantitative comparison of FT-IR data is difficult, peak areas attained using spectral deconvolution were internally correlated to quantify relative changes in CO adsorption on various sites, similar to the type of analysis reported by others [24,25]; however, it is important to realize that the analysis results are based on the assumptions that: (1) there is no intensity borrowing from dipole coupling effects, (2) the bands vary linearly with CO coverage, and that, (3) the extinction coefficients are similar for similar surface species. Data in Table 1 show that deposition of Cu on the two different linear sites and the two different three-fold hollow sites occurs at different rates as illustrated in Fig. 7. The L2/L1 (linear high frequency peak/linear low frequency peak) ratio decreases with increasing Cu loading, suggesting that initial Cu deposition may preferentially occur on specific edge and corner sites,

Table 1
Summary of spectral deconvolution results

| Sample | Cu coverage (ML) | Maxima for deconvoluted peaks | | | | | Ratio of peak areas | |
|---|---|---|---|---|---|---|---|---|
| | | Log-normal H1 ($cm^{-1}$) | Gaussian H2 ($cm^{-1}$) | Log-normal B1 ($cm^{-1}$) | Log-normal L1 ($cm^{-1}$) | Gaussian L2 ($cm^{-1}$) | L2/L1 | H2/H1 |
| $Pd/SiO_2$ | 0 | 1882 | 1907 | 1979 | 2074 | 2088 | 0.21 | 0.04 |
| 0.17 wt.% Cu[a] | 0.37 | 1880 | 1911 | 1976 | 2069 | 2087 | 0.20 | 0.02 |
| 0.32 wt.% Cu[a] | 0.61 | 1880 | 1909 | 1976 | 2066 | 2086 | 0.10 | 0.01 |
| 0.60 wt.% Cu[a] | 0.90 | 1859 | 1907 | 1969 | 2032 | 2071 | [b] | 0.02 |

L: linearly bonded; B: bridged bonded; H: three-fold hollow bonded CO on Pd.
[a] Cu loading on $Pd/SiO_2$.
[b] The broad, featureless nature of this peak caused the fitting to be difficult, and the resultant areas were considered unreliable.

Table 2
Summary of catalyst performance for EpB hydrogenation including conversion and product selectivity

| Sample | Cu coverage (ML)[a] | EpB conversion (%) | Selectivity (%) | | | | | | |
|---|---|---|---|---|---|---|---|---|---|
| | | | BO[b] | *n*-Butanal | *n*-Butanol | 3-Buten-1-ol | 2-Butenal | 2-Buten-1-ol | Unsaturated C=C[c] |
| $Pd/SiO_2$ | 0.00 | 24.9 | 9.7 | 36.4 | 4.3 | 3.1 | 41.8 | 4.6 | 49.5 |
| 0.17 wt.% Cu[a] | 0.37 | 34.7 | 10.4 | 13.1 | 1.9 | 13.9 | 53.5 | 7.4 | 74.8 |
| 0.32 wt.% Cu[a] | 0.61 | 43.7 | 10.1 | 13.7 | 9.2 | 13.1 | 44.3 | 9.4 | 66.8 |
| 0.60 wt.% Cu[a] | 0.90 | 29.4 | 11.0 | 21.3 | 11.3 | 10.9 | 35.8 | 10.3 | 57.0 |

[a] Cu coverage calculated from CO chemisorption data as noted in text.
[b] BO is an abbreviation for butylene oxide (1,2-epoxybutane).
[c] Unsaturated C=C includes 3-buten-1-ol, 2-butenal, and 2-buten-1-ol.

inhibiting CO adsorption at these sites (~2085 $cm^{-1}$). Similarly, the H2/H1 (high frequency three-fold peak/low frequency three-fold peak) ratio decreases with increasing Cu loading, suggesting that initial deposition of Cu preferentially occurs on the high frequency three-fold hollow sites (~1910 $cm^{-1}$).

Interestingly, Melendrez et al. [25] prepared Cu–Pd bimetallic catalysts using both hydrogen redox and coimpregnation methods and found there were different preferences for Cu placement (based on FT-IR profiles of CO adsorption) for each method of preparation. Thus, it is not surprising that Cu has been reported to exhibit placement on Pd surfaces ranging from random to highly preferential in nature [24,25].

Steady state catalyst performance data (minimum of 6 h of time on-line) for EpB hydrogenation for several of the Cu–Pd/$SiO_2$ catalysts are summarized in Table 2. Reaction conditions used for all catalysts were 323 K reaction temperature and a feed composition of 2.5% EpB, 10% $H_2$, and balance He at a GHSV = 320,000 $h^{-1}$. Conversion of EpB was intentionally maintained at <100% conversion to determine the effects of catalyst composition on overall activity. The overall product distribution in Table 2 is better explained by examination of the overall reaction scheme in Fig. 8 for EpB hydrogenation over Rh catalysts [9–12]. While this reaction scheme may not be totally valid for Pd-based catalysts, the studies of Bartok et al. [6] for the hydrogenation of EpB over $Pd/SiO_2$ catalysts suggest

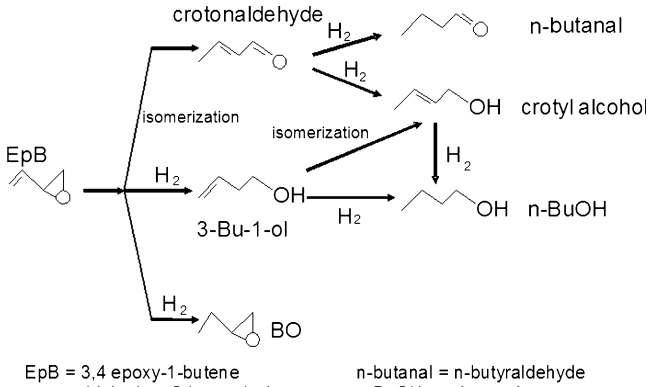


Fig. 8. Reaction pathways for the hydrogenation of EpB over supported Rh catalysts. Data adapted from results in Refs. [9–12]. Compounds are identified in terms of both IUPAC nomenclature as well as commonly used names.

many common features. The reaction scheme in Fig. 8 indicates a three-way parallel reaction network, leading to the formation of epoxybutane, *n*-butanal, and *n*-butanol as stable end products. The unsaturated C=C products, 2-butenal, 3-buten-1-ol, and 2-buten-1-ol are all intermediates leading to the formation of *n*-butanal and *n*-butanol. At similar reaction conditions, Bartok et al. [6] also found that epoxybutane and *n*-butanal were formed by separate reaction pathways; *n*-butanol was not observed as a reaction product. The results in Table 2 for $Pd/SiO_2$ show the formation of both epoxybutane and *n*-butanal (in approximately the same ratio as observed by Bartok et al. [6]); however, the $Pd/SiO_2$ catalyst in this study does produce *n*-butanol, 3-buten-1-ol, and 2-buten-1-ol, the latter two products almost certainly being intermediates for *n*-butanol formation. Isomerization of EpB to 2-butenal is also observed in our evaluations and is very likely an intermediate leading to Pd-catalyzed formation of *n*-butanal as noted by Bartok et al. [6].

Bartok et al. [7] have also evaluated a 6.4 wt.% $Cu/SiO_2$ catalyst for EpB hydrogenation and found that the primary reaction products were essentially limited to 1,3-butadiene and 2-butenal. The latter was formed by the isomerization of EpB to the more thermodynamically-stable α,β-unsaturated aldehyde, while 1,3-butadiene was formed by the thermodynamically-favored reaction of EpB with $Cu^0$ sites to form an oxidized Cu site and 1,3-butadiene. This is in agreement with the results of Monnier and Hartley [52] for the interaction of EpB with Cu/α-$Al_2O_3$ catalysts. The fact that the $\theta_{Cu} = 0.9$ catalyst in Table 2 produced substantial amounts of epoxybutane and *n*-butanal, indicative of Pd catalysts and not of $Cu/SiO_2$ catalysts, confirms that the Cu coverage on Pd is not monodisperse and agrees well with the CO chemisorption data. Further, the fact that 1,3-butadiene was formed only in trace amounts for the catalysts in this study indicates that the Cu present in the $\theta_{Cu} = 0.9$ catalyst was not present as typical supported $Cu^0$ particles.

The data in Fig. 9 show more clearly the trends of increasing Cu loadings on catalyst performance. Due to the ability of Pd to stabilize the π-allylic, ring-opened intermediate of EpB [53], the selectivity of Pd-catalyzed hydrogenation to epoxybutane is relatively low at ~10–11% regardless of Cu content. As noted above, epoxybutane formation is not observed over normal supported Cu catalysts [7]. However, the overall rate of epoxybutane formation does pass through a maximum at intermediate Cu coverages (selectivity to epoxybuta-

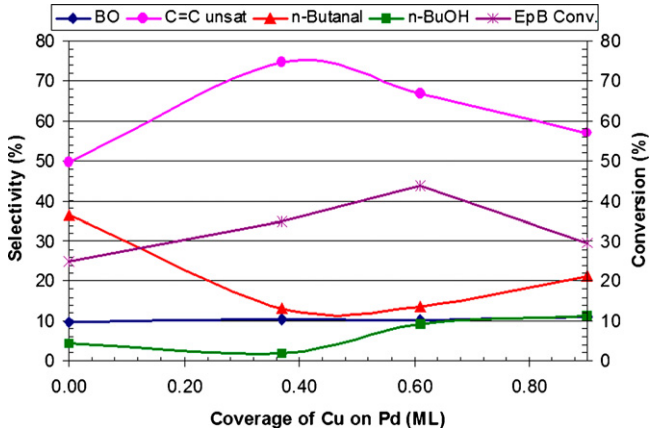


Fig. 9. Effects of Cu coverage on Pd for the hydrogenation of EpB. Cu coverage was calculated as defined in the text.

ne × conversion), indicating a mild structure sensitivity for this reaction. Further, the constant selectivity for epoxybutane formation also requires a constant selectivity to products formed by ring-opening, suggesting that only small Pd ensembles are required for the ring-opening reaction.

The other notable feature of catalyst performance in Fig. 9 is that formation of all unsaturated intermediates is greatest for intermediate Cu coverages. Copper catalysts have been used for selective hydrogenation of unsaturated aldehydes to form unsaturated alcohols [54], and supported Pd catalysts are typically not good catalysts for the selective reduction of C=O groups [55,56]. For example, Ashour et al. [42] have studied hydrogenation of 2-butenal at 383 K over bimetallic Cu–Pd catalysts prepared by simultaneous impregnation of Cu and Pd salts and compared the activities with those for conventionally prepared $Cu/SiO_2$ and $Pd/SiO_2$ catalysts. They observed a high (64%) selectivity to 2-buten-1-ol (crotyl alcohol) over $Cu/SiO_2$; other reported products included lesser amounts of *n*-butanal and *n*-butanol, indicating an overall preference of Cu catalysts for the reduction of C=O bonds to form the corresponding alcohol. Further, Ashour reported 0% selectivity to 2-buten-1-ol for bimetallic catalysts having high molar ratios of Pd to Cu, consistent with the observed increases in 2-buten-1-ol selectivity with higher Cu loadings summarized in Table 2. Finally, Hubaut et al. [8] also examined gas phase hydrogenation of crotonaldehyde over $Cu/Cr_2O_3$ at 313 K and reported data suggesting that *n*-butanal underwent further hydrogenation to form *n*-butanol. The formation of *n*-butanol by Cu catalyzed C=O hydrogenation could explain the observed overall increase in the selectivity to *n*-butanol (4.3–11.3%) in Table 2 for increasing Cu loadings. However, in our study, the highest selectivity to unsaturated intermediates in Fig. 9 is not at the highest Cu coverages, but at intermediate coverages.

These above trends suggest the existence of bimetallic Cu–Pd sites that activate EpB in such a way that both conversion of EpB and selectivity to C=C unsaturated intermediates are increased. Electronic effects between Cu and Pd are reportedly small [38,42], and the existence of Pd ensemble effects that, in this case, promote the formation of epoxybutane should result in lower selectivities for the formation of C–O epoxy ring-opened products, since hydrogenolysis reactions typically involve larger metal ensembles than those required for simple C=C hydrogenation reactions. However, the results in Table 2 indicate this is not the case. Therefore, Cu must be involved in the hydrogenolysis reaction over the same range of Cu loadings. Thus, the observed effects of Cu deposition on Pd with respect to C–O hydrogenolysis are perhaps more indicative of the reactivity of bifunctional Cu–Pd sites. Based on the oxophilic nature of Cu [7,8,52], the Cu portion could function to activate the epoxy end of the EpB molecules towards ring opening, while the Pd site stabilizes the terminal, π-allylic [53] portion of the adsorbed intermediate. Controlled hydrogenation of this adsorbed intermediate should result in the formation of unsaturated alcohols and aldehydes due to the selectivity of Cu sites for C=O bond hydrogenation. Existence of such Cu–Pd sites would both increase the overall rate of EpB conversion as well as the selectivity for the formation of unsaturated alcohols and aldehydes. Based on the catalyst performance curves in Fig. 9, the surface concentration of these bifunctional Cu–Pd sites are, not unexpectedly, highest at intermediate Cu coverages on the Pd surface. As a corollary, based on density functional theory calculations for the Cu and Pd bimetallic system, Groβ [57] concluded that the strong interaction between Cu and Pd should lead to the formation of a pair-wise interaction to give a new catalytic site having properties intermediate to the properties of the individual metallic components [57].

One final explanation for the observed reaction trends is that electrolessly deposited Cu may be dissolved in the Pd lattice of the Pd crystallites, strongly modifying the catalytic properties of the surface Pd sites. It is known [14,58] that Pd and Cu form a continuous series of solid solutions whose surface composition closely mirrors that of the bulk composition. Although, these bimetallic alloys, or solid solutions, are typically formed by high temperature treatments (>1073 K) of the two component solid mixtures, alloy formation has been speculated for catalysts prepared at temperatures as low as 523 K [42]. The Cu–Pd bimetallic particles in this study were initially formed at 296 K and were exposed to temperatures ≤373 K during pretreatment and catalyst evaluation. Therefore, it is highly unlikely that the Cu–Pd bimetallic particles in this study are indicative of high temperature, Cu–Pd bulk alloy compositions.

## 4. Conclusions

Electroless deposition has been used to prepare a family of Cu–Pd bimetallic catalysts whereby the deposition of Cu is limited only to the pre-existing Pd surface. The loading of the Cu component on the Pd surface can be systematically varied by modification of the kinetic parameters controlling electroless deposition, namely, deposition temperature, concentrations of the HCHO reducing agent and the $Cu^{2+}$ salt, and deposition time. Using deposition time as the kinetic variable, a series of Cu–Pd bimetallic catalysts having different Cu loadings have been prepared and evaluated for the hydrogenation of 3,4-epoxy-1-butene, a functionalized olefin having many potential reaction pathways. Catalyst performance and characterization

results suggest that Cu is not distributed in a monodisperse manner on the Pd surface, indicating the existence of autocatalytic deposition of Cu on Cu surfaces. FT-IR data suggest that initial Cu deposition occurs preferentially on specific low coordination, surface Pd sites and on specific three-fold hollow Pd(1 1 1) sites, although Cu deposition led to a decrease in CO adsorption on all surface Pd sites. The bimetallic Cu–Pd sites that are formed exhibit unusually high activity for EpB conversion and selectivity towards unsaturated alcohols and aldehydes. This bimetallic effect on catalyst activity and selectivity is best explained, not by the existence of either ligand or ensemble effects, but rather by the bifunctional nature of the Cu–Pd sites present on the surface of these catalysts. Finally, in a more general sense, we have demonstrated that electroless deposition is capable of providing a wide range of bimetallic catalysts having specific surface compositions.

## Acknowledgements

This research project was supported financially by the University of South Carolina Nanocenter and NSF Grant no. 0456899. The authors also gratefully acknowledge Engelhard Corporation for supplying the $Pd/SiO_2$ base catalyst and Eastman Chemical Company for supplying the EpB used in this study. One of us (JRM) would also like to acknowledge Professor Al Vannice for the many years of interaction and mentoring that have contributed to JRM's career.

## References

[1] P.N. Rylander, Catalytic Hydrogenation in Organic Syntheses, Academic Press, New York, 1979.
[2] P.N. Rylander, Hydrogenation Methods, Academic Press, New York, 1985.
[3] F. Delbecq, P. Sautet, J. Catal. 152 (1995) 217.
[4] N. Ravasi, M. Rossi, J. Org. Chem. 56 (1991) 4329.
[5] J.A. Cabello, J.M. Campelo, A. Garcia, D. Luna, J.M. Marinas, J. Mol. Catal. 67 (1991) 217.
[6] M. Bartok, A. Fasi, F. Notheisz, J. Catal. 175 (1998) 40.
[7] M. Bartok, A. Fasi, F. Notheisz, J. Mol. Catal. A: Chem. 135 (1998) 307.
[8] R. Hubaut, M. Daage, J.P. Bonnelle, Appl. Catal. 22 (1986) 231.
[9] B.D. Roberts, J.R. Monnier, D.M. Hitch, US Patent 6,180,559, issued to Eastman Chemical Company (2001).
[10] B.D. Roberts, J.R. Monnier, D.M. Hitch, US Patent 6,310,223, issued to Eastman Chemical Company (2001).
[11] S.N. Falling, US Patent 5,077,418, issued to Eastman Chemical Company (1991).
[12] H. Fujitsu, E. Matsumura, S. Shirahama, K. Takeshita, I. Mochida, J. Chem. Soc., Perkin I (1982) 855.
[13] S. Cho, B. Lee, H. Alper, Tetrahedron Lett. 36 (1995) 6009.
[14] R.L. Moss, L. Whalley, Adv. Catal. 22 (1972) 115.
[15] W.M.H. Sachtler, Catal. Rev. Sci. Eng. 14 (1976) 193.
[16] J.H. Sinfelt, Acc. Chem. Res. 10 (1977) 15.
[17] R. Burch, J.C.S. Chem. Commun. (1981) 845.
[18] V. Ponec, Appl. Catal. A: Gen. 222 (2001) 31.
[19] G. Ertl, H. Knozinger, J. Weitkamp (Eds.), Handbook of Heterogeneous Catalysis, vol. 1, VCH Press, Weinheim, 1997, pp. 191–286.
[20] F. Nagy, S. Szabo, React. Kinet. Catal. Lett. 35 (1987) 133.
[21] S.S. Djokic, Mod. Asp. Electrochem. 35 (2002) 51.
[22] Y. Okinaka, T. Osaka, Adv. Electrochem. Sci. Eng. 3 (1994) 55.
[23] M. Paunovic, in: O.J. Murphy, S. Srinivasan, B.E. Conway (Eds.), Electrochemical Transitions, Plenum Press, New York, 1992, p. 479.
[24] F. Gauthard, F. Epron, J. Barbier, J. Catal. 220 (2003) 182.
[25] R. Melendrez, G. Del Angel, V. Bertin, M.A. Valenzuela, J. Barbier, J. Mol. Catal. A: Chem. 157 (2000) 143.
[26] H.-F. Chang, M. Abu Saleque, W.-S. Hsu, W.-H. Lin, J. Mol. Catal. A: Chem. 109 (1996) 249.
[27] R.F. Hicks, Q.-J. Yen, A.T. Bell, J. Catal. 89 (1984) 498.
[28] S. Lambert, B. Heinrichs, A. Brasseur, A. Rulmont, J.-P. Pirard, Appl. Catal. A: Gen. 270 (2004) 201.
[29] J.R. Monnier, M.J. Hanrahan, G. Apai, J. Catal. 92 (1985) 119.
[30] J.R. Monnier, J.W. Medlin, M.A. Barteau, J. Catal. 203 (2001) 362.
[31] J.R. Monnier, K.T. Peters, G.W. Hartley, J. Catal. 225 (2004) 374.
[32] H. Akahoshi, K. Murakami, M. Wajima, S. Kawakubo, IEEE Trans. Comp. Hybrids Manuf. Tech., CHMT-9 (1986) 181.
[33] C. Kerr, D. Barker, F. Walsh, Trans. IMF 79 (2001) 41.
[34] A. Molenaar, M.F.E. Holdrinet, I.K.H. Van Beek, Plating 60 (1973) 635.
[35] B.J. Feldmann, O.R. Melroy, J. Electrochem. Soc. 136 (1989) 640.
[36] K.G. Wiese, K.G. Weil, Ber. Bunsenges Phys. Chem. 91 (1987) 619.
[37] Y. Shacham-Diamand, V.M. Dubin, Microelectron. Eng. 33 (1997) 47.
[38] F. Skoda, M.P. Astier, G.M. Pajonk, M. Primet, Catal. Lett. 29 (1994) 159.
[39] J.B. Giorgi, T. Schroeder, M. Bäumer, H.-J. Freund, Surf. Sci. 498 (2002) L71.
[40] J.R. Monnier, J.W. Medlin, Y.-J. Kuo, Appl. Catal. A: Gen. 194–195 (2000) 463.
[41] H. Unterhalt, G. Rupprechter, H.-J. Freund, J. Phys. Chem. B 106 (2002) 356.
[42] S.S. Ashour, J.E. Bailie, C.H. Rochester, J. Thomson, G.J. Hutchings, J. Mol. Catal. A: Chem. 123 (1997) 65.
[43] T. Gieβel, O. Schaff, C.J. Hirschmugl, V. Fernandez, K.-M. Schindler, A. Theobald, S. Bao, R. Lindsay, W. Berndt, A.M. Bradshaw, C. Baddeley, A.F. Lee, R.M. Lambert, D.P. Woodruff, Surf. Sci. 406 (1998) 90.
[44] P. Gelin, A.R. Siedle, J.T. Yates Jr., J. Phys. Chem. 88 (1984) 2978.
[45] T. Wadayama, Y. Sasaki, K. Shiomitsu, A. Hatta, Surf. Sci. 592 (2005) 72.
[46] S. Bertarione, D. Scarano, A. Zecchina, V. Johánek, J. Hoffmann, S. Schauermann, M.M. Frank, J. Libuda, G. Rupprechter, H.-J. Freund, J. Phys. Chem. B 108 (2004) 3603.
[47] K. Kolasinski, Surface Science—Foundations of Catalysis and Nanoscience, John Wiley and Sons, West Sussex, 2002.
[48] C.-S. Chen, J.-H. Lin, H.-W. Chen, Appl. Catal. A: Gen. 298 (2006) 161.
[49] R. Van Hardeveld, F. Hartog, Surf. Sci. 15 (1969) 189.
[50] J. Szanyi, W.K. Kuhn, D.W. Goodman, J. Vac. Sci. Technol. A 11 (1993) 1969.
[51] W.K. Kuhn, J. Szanyi, D.W. Goodman, Surf. Sci. 274 (1992) L611.
[52] J.R. Monnier, G.W. Hartley, J. Catal. 203 (2001) 253.
[53] S.A. Godleski, in: B.M. Trost (Ed.), Comprehensive Organic Synthesis, Pergamon Press, New York, 1991, pp. 585–663.
[54] A. Dandekar, R.T.K. Baker, M.A. Vannice, J. Catal. 184 (1999) 421.
[55] V. Ponec, Appl. Catal. A: Gen. 149 (1997) 27.
[56] P.N. Rylander, Catalytic Hydrogenation over Platinum Metals, Academic Press, New York, 1967, p. 250.
[57] A. Groβ, Topics Catal. 37 (2006) 29.
[58] G.A. Kok, A. Noordermeer, B.E. Nieuwenhuys, Surf. Sci. 152/153 (1985) 505.